The Effect of Decision Analysis on Power System Resilience and Economic Value During a Severe Weather Event

Yuan-Kang Wu, *Member, IEEE*, Yu-Chih Chen, Hui-Ling Chang, and Jing-Shan Hong

***Abstract*—Because of climate changes, natural disasters are becoming more serious. For instance, the intensity of typhoons has been increasing in recent years. Typhoons and other natural disasters have high-impact low-probability characteristics. Thus, procedures for preparing for natural disasters and increasing power system resilience are important issues. This article proposes an all-inclusive process for system operators to make decisions for enhancing power system resilience and economic value during a severe weather event. This process first considers the typhoon track, the fragility curve and the recovery time of transmission lines. After collecting these data, system simulations and a calculated resilience index are implemented according to cases with and without disaster prevention. Next, the probability threshold and calculated economic value index are obtained based on numerical weather prediction wind speeds and the cost-loss ratio. Finally, the two indexes are considered in combination to obtain the highest resilience with the greatest benefit. The proposed process helps system operators make decisions for appropriate preventive actions at the least cost. An actual Taiwan power system and a severe weather event are used as an example to demonstrate the proposed decision analysis. The simulation results indicate the feasibility of the proposed method, which can reduce potential risks caused by extreme weather events with the maximum economic benefits.**

***Index Terms*—Decision analysis, economic value (EV), high-impact low-probability (HILP), preventive action, resilience, severe weather event, typhoon.**

I. Introduction

POWER system security has become more important in modern power grids. However, many natural disasters, such as typhoons and earthquakes are unavoidable and often cause large-scale power failures. Such disasters are called high-impact but low-probability (HILP) events [1], [2]. Because of climate change, the intensity of typhoons is increasing. The probability of occurrence of supertyphoons has increased and these are accompanied by record-breaking wind speeds. The superhigh wind speeds can cause destruction of electricity towers and transmission lines, leading to the collapse of power grids. In addition, extreme wind speeds can cause part of a power grid to be separated from the main grid and thus increase economic losses [3].

To prepare for unavoidable HILP events, system operators need to pay more attention to the resilience of their power systems. This includes increasing the flexibility of a power system to respond to HILP events. It is of primary importance that system operators use a resilience index to quantify power system resilience [4]. The resilience index is calculated by considering system loads, the effect time of a typhoon, and the system recovery time. This index can be used to compare the abilities of different power systems to respond to extreme HILP events. The resilience index is typically based on the supplier's load before and after a failure, since electricity supply to several system loads cannot be met during an event. That is, the resilience index represents the area under a load-time curve using an integral method [5], [6]. More sophisticated resilience indices consider the effect time of an event and the recovery time of a power system [7], [8].

Power system resilience can be enhanced using different preventive actions and reinforcements. One strategy for enhancing power system resilience is to reduce supply loss during extreme HILP events [9]. Numerous studies have proposed a variety of methods to improve power system resilience, as summarized in Fig. 1. These methods include the use of storage systems, development and control of microgrids, implementation of preventive action strategies, planning of restoration processes, and long-term resilience-oriented system planning. For example, Kosai and Cravioto [10] and Nazemi *et al.* [11] highlighted the importance of energy storage system (ESS) on the improvement of power system resilience. With an appropriate design, power from ESSs can be quickly supplied to consumers after a natural disaster. Improved system resilience through grid-connected ESSs has been demonstrated [12]. For instance, if an extreme event is expected to occur, then ESSs can be charged before the disaster strikes. As a typhoon can cause disconnection of lines and several islanding parts in a power system, ESSs can be used for supporting power supply at such times. Renewable energy can also be stored in advance to extend the duration

Manuscript received July 31, 2021; revised October 16, 2021; accepted October 20, 2021. Date of publication January 25, 2022; date of current version March 20, 2022. Paper 2021-PSEC-0869.R1, presented at the IEEE Industry Applications Society Annual Meeting, Vancouver, BC Canada, Oct. 10–14, and approved for publication in the IEEE TRANSACTIONS ON INDUSTRY APPLICATIONS by the Power Systems Engineering Committee of the IEEE Industry Applications Society. *(Corresponding author: Yuan-Kang Wu.)*

Yuan-Kang Wu and Yu-Chih Chen are with the National Chung-Cheng University, Chia-Yi 62102, Taiwan (e-mail: allenwu@ccu.edu.tw; rongjojo@gmail.com).

Hui-Ling Chang and Jing-Shan Hong are with the Meteorological Information Center, Central Weather Bureau, Taipei 10048, Taiwan (e-mail: lingo@cwb.gov.tw; rfs14@cwb.gov.tw).

Color versions of one or more figures in this article are available at https://doi.org/10.1109/TIA.2022.3145753.

Digital Object Identifier 10.1109/TIA.2022.3145753

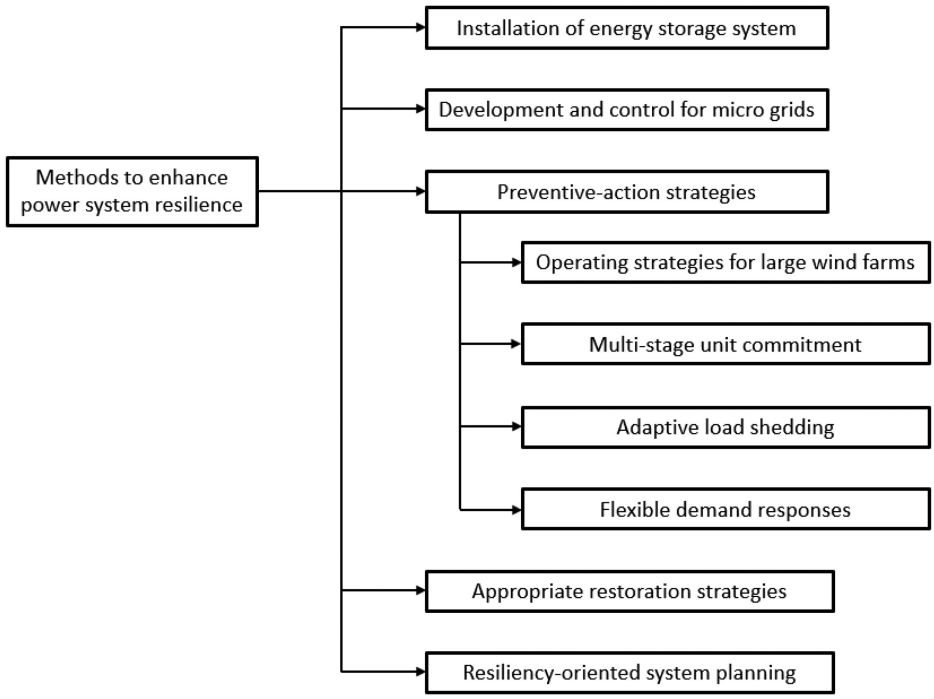

Fig. 1. Methods to enhance power system resilience.

of power supply. For example, solar panels on buildings can support electricity when extreme events occur, thus improving power system resilience [13].

Microgrid control is another strategy to improve power system resilience. For instance, when a typhoon approaches, a power system can be divided into several microgrids in advance that can be controlled separately, thus avoiding large-scale power failures [14]–[16]. Operation planning for such microgrids can resolve severe power outages [17].

Numerous preventive action strategies have been proposed to enhance power system resilience. These strategies cover wind farm operation, unit scheduling, load shedding and demand response. Many offshore wind farms have been installed to replace traditional thermal generators and the operation of these offshore wind turbines could be severely affected by typhoons. Thus, appropriate operating strategies for offshore wind turbines are important. An optimal cut-off scheduling for wind turbines before a typhoon strikes has been proposed [18], in which the cut-off sequence and corresponding wind speeds are required to match the ramping rates of thermal and hydraulic units. Appropriate preventive actions in offshore wind farms can mitigate reduction in power generation caused by the abrupt shutdown of wind turbines during excessive wind speeds. If typhoon wind-speed forecasts are accurate, then system operators can increase system resilience through advanced unit scheduling [19]. Dhiman *et al.* [20] indicated that the operation and maintenance cost of wind turbines are significant factors in wind farm operation, and that data-driven condition monitoring can increase the reliability of wind power systems; thus, the study in [20] proposed an adaptive AI method to detect abnormal operations in wind turbines to improve system resilience.

Preventive actions on unit scheduling, network reconfiguration, and load-shedding schemes have also been proposed. Owing to the uncertainties of typhoon tracks and line outages, Ding *et al.* [21] developed a three-stage unit commitment model to improve power system resilience. The model included preventive control (adjustment of generation units), emergency control (load shedding), and a restoration strategy. Li *et al.* [22] also developed a protective strategy to increase system resilience by reconstructing system topology and controlling load demands when a storm approaches.

In the future, the number of electric vehicles will increase. These electric vehicles can be regarded as one of the power supplies in microgrids, and they can combine diesel generators and solar energy to supply critical loads and enhance system resilience. Momen *et al.* [23] proposed a two-stage stochastic framework that considers the charging and discharging of electric vehicles, diesel generators, and solar energy to greatly increase the supplied load.

For long-term power system planning, several works have proposed resiliency-oriented system planning to build transmission systems or distributed generators. For example, Ranjbar *et al.* [24] proposed a system planning that considers normal and emergency conditions with different maintenance times, which significantly reduces load-shedding and increases system resilience.

In addition, power system operators can evaluate potential benefits when making operating decisions. Therefore, implementing economic value analyses is important. The purpose of this is to quantify the economic benefits based on probabilistic forecasts. This article uses numerical weather prediction (NWP) forecasts made by the Central Weather Bureau of Taiwan to

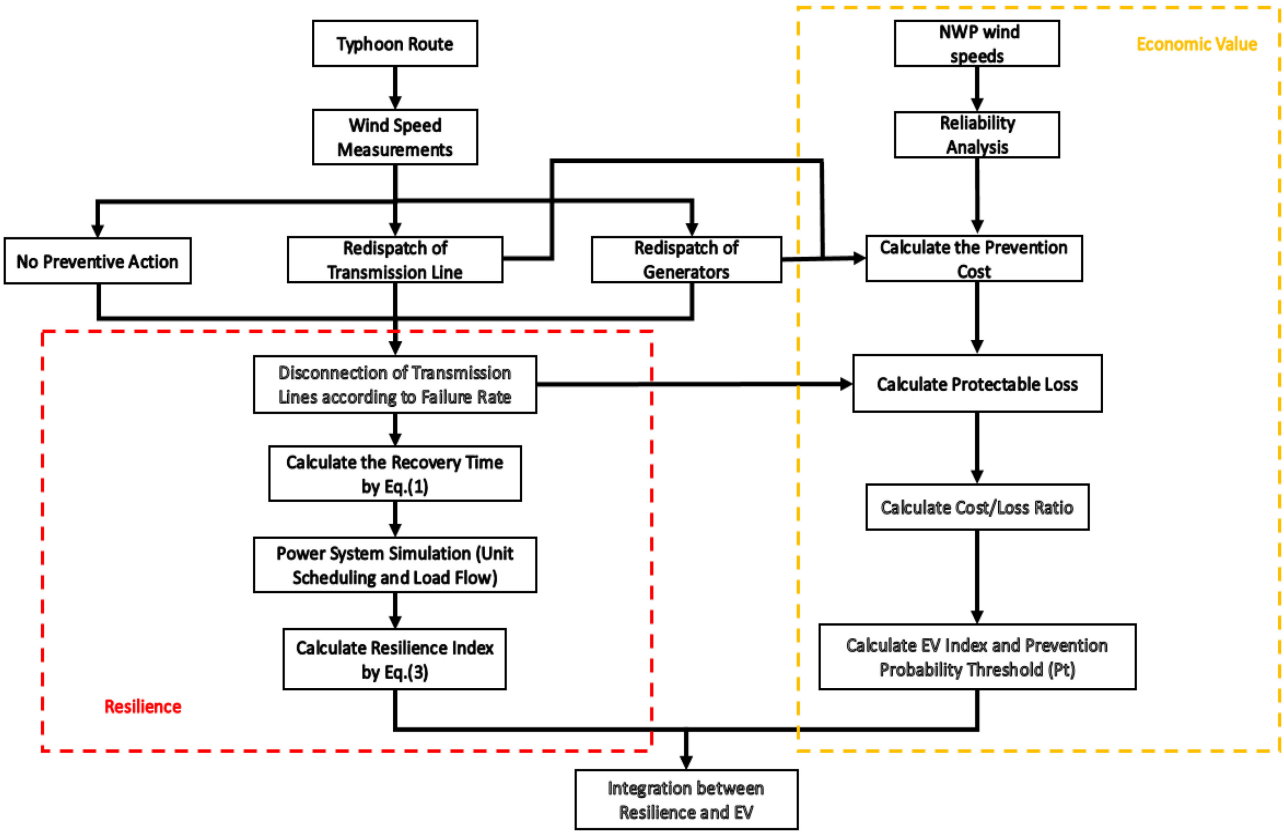

Fig. 2. Flowchart of this article.

explore whether the proposed preventive actions during severe weather events have economic value.

Although previous works have proposed several methods to calculate power system resilience, most have only considered small testing systems as examples. In addition, most previous studies have concentrated on the improvement of system resilience, and do not consider economic evaluations of preventive actions. In a power system, operators should select appropriate preventive actions with the lowest cost and the greatest benefit. Therefore, this article considers both system resilience and economic value to improve the system performance. Fig. 2 shows the complete flow chart for this article. The process on the left-hand side is used to calculate power system resilience. First, system operators are required to collect the typhoon track and wind-speed data. Next, system operators should consider different operating scenarios, i.e., with or without preventive actions, to implement power system simulations, in which transmission line outages and their recovery times are also considered. Finally, system resilience values under different operating scenarios are obtained.

The process on the right-hand side of Fig. 2 is used to calculate EV. Its main steps include reliability analyses for NWPs and calculations of prevention cost, protectable loss, and cost-loss ratio. Finally, the economic value and prevention probability threshold are obtained.

In the last step, both resilience value and economic value are integrated to evaluate the feasibility of the proposed preventive actions. The main contributions of this article are as follows.

1) This article considers both resilience and economic values, which helps system operators make decisions for appropriate preventive actions at the least cost.
2) This article uses a real power system and a severe weather event as an example to demonstrate the proposed decision analysis.
3) This article considers different preventive actions to improve power system resilience and compares the simulation results, providing a significant reference for selecting preventive actions.
4) This article provides a clear suggestion for when preventive actions should start and indicates the maximum economic value.

Section II introduces the fragility curve of a transmission line, system recovery time, and the calculation of resilience index. Section III describes the method used to calculate the economic value index. Section IV presents a case study to demonstrate the proposed process for decision analysis of power system resilience and economic value during a severe weather event and Section V draws the conclusion.

II. Calculation of Resilience Index Based on Line Failure Model

To calculate the resilience index of a power system when a typhoon approaches, the first step is to investigate the typical failure curve of a transmission line, i.e., the influence of wind speeds on the failure rate of a transmission line. The greater the

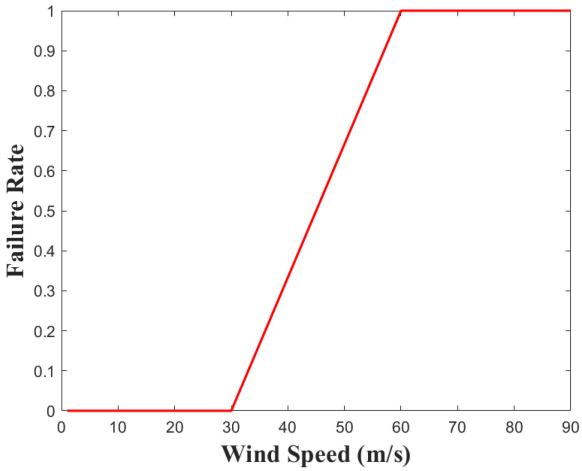

Fig. 3. Fragility curve of a transmission line.

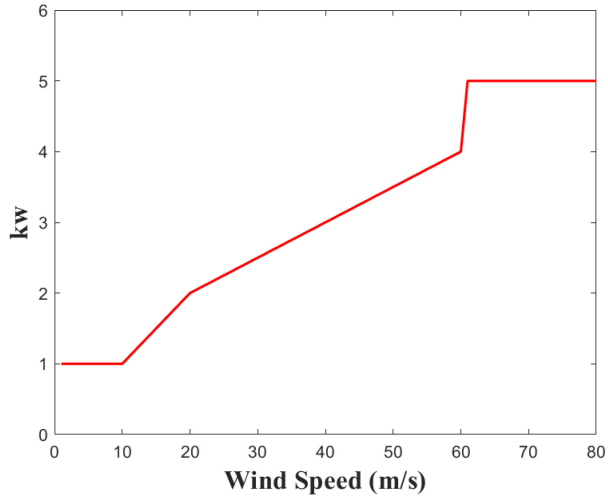

Fig. 4. Schematic diagram of k_w.

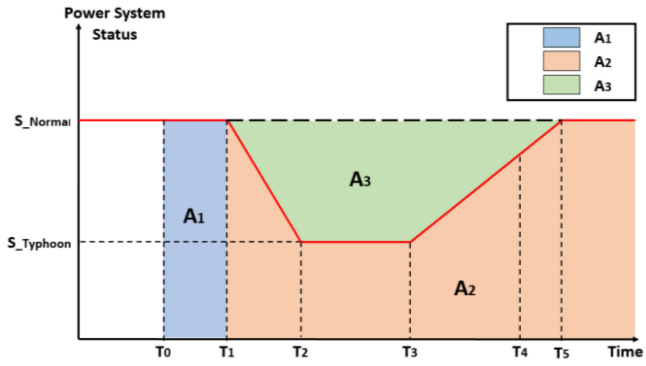

Fig. 5. Schematic diagram of system status.

wind speed, the greater the probability of line disconnection. Different wind speeds cause different failure probabilities of a transmission line. The second step is to investigate the recovery time of a failure transmission line. Generally, the recovery time is based on the length of a transmission line, failure probability, and wind speeds. The last step is to calculate the resilience index of the analyzed power system, reflecting the ability of the system to respond to typhoons.

A. Fragility Curve of Transmission Lines

To simulate the impact of a typhoon on power systems, it is necessary to consider the possible disconnection of transmission lines caused by strong wind speeds, which reflects the damages to power systems. Owing to line outage, many buses in the system are forced to be disconnected from the main grid, causing the loss of load demand. Thus, the definition of the fragility curve of a transmission line is important and will affect the simulation result. Fig. 3 shows the fragility curve used in this article. The fragility curve (see Fig. 3) is based on Fig. 1 of Li *et al.* [22], which is used to indicate the influence of different wind speeds on the outage of lines. The greater the wind speed, the greater the damage to the line, so the probability of line failure increases. Fig. 3 provides a clear and simple relationship between wind speed and failure rate, which is suitable for industry applications.

B. Recovery Time of Transmission Line

After a transmission line is disconnected, the time to recover (TTR) should be counted. TTR is typically used to indicate when a transmission line is reconnected to the system during line failure. The following equation is used to calculate TTR [7]

$$\text{TTR} = (\text{length of line} \times 2) \times \text{failure rate} \times k_w. \quad (1)$$

This article assumed that the TTR of a 500-m transmission line is 1 h. Additionally, the probability of line disconnection is based on the fragility curve; that is, the high wind speeds of a typhoon lead to a high probability of line disconnection. In (1), k_w represents different factors for recovery time under different wind speeds. For example, high wind speeds cause serious damages to lines, thus increasing the recovery time of transmission lines. In other words, k_w represents the parameter that describes the relationship between wind speeds and the recovery times of lines. The different k_w settings based on different wind-speed ranges are given below and depicted in Fig. 4

$$k_w = \begin{cases} 1 & 0 \le v \le 10\,\text{m/s} \\ U(1,2) & 10\,\text{m/s} < v \le 20\,\text{m/s} \\ U(2,3) & 20\,\text{m/s} < v \le 40\,\text{m/s} \\ U(3,4) & 40\,\text{m/s} < v \le 60\,\text{m/s} \\ U(4,5) & 60\,\text{m/s} < v \end{cases}. \quad (2)$$

The values of k_w are based on [7, eq. (13)], which is used to reflect the influence of different wind speeds on the maintenance time. High wind speeds cause more damages to transmission lines, and thus extend the maintenance time needed for them.

C. Calculation of Resilience Index

This section introduces the method used to calculate power system resilience. Fig. 5 shows a schematic diagram of system changes when the power system experiences a typhoon.

This article calculated the resilience index using the method of [7], where T_0 is the time when a typhoon starts to impact the

power system, T_1 is the time when transmission lines disconnect and some loads are shed, resulting in a drop in the load demand of the system. The time from T_2 to T_3 is the minimum load during the typhoon, and after T_3 transmission lines will be reconnected successively to the main grid. At T_4, the typhoon has passed and no longer has an effect on the system. Finally, T_5 is the time when the power system returns to normal. According to the different system statuses, the area in Fig. 5 can be divided into the A_1 (blue), A_2 (pink), and A_3 (green) regions: A_1 is the supplied load when the system is in normal operation during the typhoon, A_2 is the supplied load when some of the transmission lines are disconnected from the main grid during the typhoon, and A_3 is the loss of supplied load caused by the typhoon.

The resilience index [7] can be calculated using

$$R = \left[\frac{A_1 + A_2}{A_1 + A_2 + A_3} \times \frac{T_{\text{dur}}}{T_5 - T_0}\right] \tag{3}$$

where T_{dur} is the impact time of the typhoon. This index can be used to compare the system resilience of different power systems during various natural disasters. The larger the area A_1, the longer the system can maintain a normal power supply during a typhoon (without a load loss). If the calculated resilience is large, then the power system has a high capability to ride through an extreme event and is more robust than other power systems. Thus, a large resilience index indicates that the power system is more robust.

To improve system resilience, area $_{.3}$ should be minimized. This article used two methods to improve power system resilience during a typhoon:

1) *Redispatch of Transmission Lines*: In this strategy, some un-activated lines in the system are activated in advance to change power flows. If a typhoon causes some line outages, then an interruption of power supply would occur in islanding systems. Therefore, redispatching transmission lines would reduce the probability of occurrence of system islanding.
2) *Redispatch of Generators*: During a typhoon, some generators would be disconnected from the main grid as result of line outages, reducing power supply in the system. Thus, several load demands must be shed, owing to insufficient power generation. Therefore, if several generators are expected to be disconnected from the grid during a typhoon, then the outputs of these generators can be reduced in advance and other generators can be redispatched to increase their power generation. That is, system operators can implement generator redispatching.

III. Calculation of Economic Value

To represent the robustness and economics of a power system in operation, this article considers both resilience and economic value. The economic value index is used to indicate whether the proposed preventive actions are economically beneficial. To calculate economic value, both wind-speed forecasts and the cost of preventive actions should be considered. Consequently, the highest economic value corresponding to a preventive action is obtained [25]–[28].

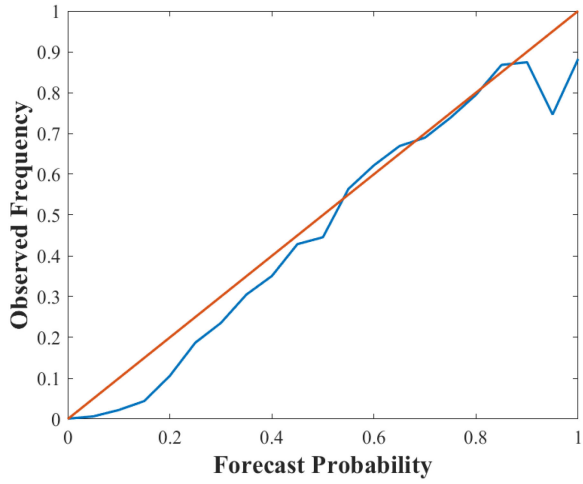

Fig. 6. Reliability analysis of wind speeds.

A. NWP Wind Speeds

The forecast wind speeds used in this article are NWP wind speeds reported by the Central Weather Bureau of Taiwan. The NWP wind speeds were produced over an area including 60 000 forecasting grids around Taiwan with 3-km model resolution and collected for typhoons from 2016 to 2019. Since the original NWPs are average wind-speed forecasts, this article collected the observed guest winds and NWP winds in 2018 over the observatory station in Taichung (near coastal in central Taiwan) and constructed their regression relation as shown in

$$y = 1.9137x + 1.359 \tag{4}$$

where x and y are average and gust wind speeds, respectively. This equation is a regression relationship derived from NWP forecasts to emphasize the influence of typhoons.

After gust wind speeds were obtained, a wind-speed threshold was set to implement a further reliability analysis. In this article, the threshold wind speed was set at 45 m/s because the probability of line disconnection at this wind speed is 50%. Fig. 6 shows the results for reliability analysis of NWP wind speeds.

Fig. 6 can be used to implement reliability analysis for NWPs. For example, when the reliability curve (blue) falls above the red diagonal line, the NWP forecast is less than the actual value, i.e., under forecasting. By contrast, when the reliability curve falls below the diagonal line, it indicates over forecasting. When the reliability curve is on the diagonal line, this represents the most ideal situation, namely that the NWP wind speeds are valid.

B. Index of Economic Value

Economic value represents potential economic benefits if the decision analysis refers to numerical forecasts [29]–[31]. For decision analysis, four scenarios should be considered.

1) A natural disaster happens, and a preventive action is taken.
2) No natural disaster happens, but a preventive action is taken.
3) A natural disaster happens, but no preventive action is taken.

TABLE I
COSTS OF FOUR SCENARIOS

Cost		Preventive action for the disaster	
		Yes	No
Disaster occurs	Yes	Scenario 1 Cost = C + Lu	Scenario 3 Cost = Lp + Lu
	No	Scenario 2 Cost = C	Scenario 4

4) No natural disaster happens, and no a preventive action is taken.

Based on the above scenarios, the expected expense for different operating situations includes the cost of preventive actions (C), the protectable loss (L_p), and the unprotectable loss (L_u) after taking preventive actions. These are further defined as follows.

1) *Cost of Preventive Actions* (C): the operating cost if a preventive action is implemented.
2) *Unprotectable Loss* (L_u): the financial loss when a natural disaster strikes a power system whether a preventive action is taken or not.
3) *Protectable Loss* (L_p): The avoidable financial loss if a preventive action is implemented before a natural disaster approaches the system. In this article, the protectable loss is regarded as the interruption cost [32].

Table I gives the operating costs corresponding to the four scenarios. It is assumed that the occurrence probability of historical disasters is $\bar{\mathrm{O}}\%$. Then, the economic value is calculated from

$$\mathrm{EV} = \frac{E_{\mathrm{climate}} - E_{\mathrm{forecast}}}{E_{\mathrm{climate}} - E_{\mathrm{perfect}}} \tag{5}$$

where E_{climate} is the cost of taking preventive actions based on historical experience, E_{perfect} is the necessary cost if the occurrence of a natural disaster can be perfectly predicted, and a natural disaster really occurs, and E_{forecast} is the cost of taking preventive actions based on NWPs.

In terms of E_{climate}, a decision maker decides to implement preventive actions based on personal experience. Thus, the preventive action is strongly related to the occurrence probability of historical natural disasters. If natural disasters occur frequently, then preventive actions will be implemented frequently. By contrast, if natural disasters rarely occur, then preventive actions are rarely performed. Therefore, the operating cost is obtained from the minimum cost of the above two situations. The formula to calculate E_{climate} is

$$E_{\mathrm{climate}} = \bar{o}\ Lu + \mathrm{Min}\left[\bar{o}Lp,\ C\right]\ . \tag{6}$$

For E_{perfect}, it is assumed that the occurrence of a natural disaster can be perfectly predicted by decision makers. Therefore, decision makers need to prescribe lower cost only if a natural disaster occurs. The formula to calculate E_{perfect} is

$$E_{\mathrm{perfect}} = \bar{o}\ (C + Lu)\,. \tag{7}$$

The optimal strategy for taking preventive actions is based on the NWPs. In such conditions, preventive actions are implemented based on the forecasting results from NWP models and the expected cost of each decision should be calculated on the basis of the probability of the four scenarios indicated above (considering the occurrence of natural disasters and the implementation of preventive actions). For example, if the occurrence probabilities of scenarios 1, 2, 3, and 4 are $h\%, f\%, m\%$ and $c\%$, respectively, then E_{forecast} can be calculated from

$$E_{\mathrm{forecast}} = h\,(C + Lu) + fC + m\,(Lp + Lu) \tag{8}$$

where the cost of scenario 4 is zero. According to (6)–(8), (5) can be transformed to

$$\mathrm{EV} = \frac{\min\left(\bar{o}, r\right) - h + fr - m}{\min\left(\bar{o}, r\right) - \bar{o}r} \tag{9}$$

where

$$r = \frac{C}{Lp}\,. \tag{10}$$

Note that EV is a relative value. As EV is equal to 1, it indicates that the prediction from the NWP models is perfect. An EV less than 0 indicates that the forecasting result from the NWP models is worse than the reference based on historical climate records or experience. In other words, system operators should implement NWP forecasts as accurately as possible and make EV close to 1 to obtain the best economic benefit.

IV. CASE STUDY

This article used Typhoon Megi as an example to demonstrate the proposed method for decision analysis. This typhoon passed through Taiwan in 2016 and caused great financial loss. Typhoon Megi initially struck Taiwan in the early morning of September 27, 2016 and passed over Taiwan that evening. Owing to its strength, high wind speeds, and high rainfall, the typhoon caused power outages in several areas. Fig. 7 shows the track of Typhoon Megi.

The track of Typhoon Megi can be divided into three stages, each with different radius of influence and wind speed according to the intensity of the typhoon. Figs. 8–10 show the three stages of the track of Typhoon Megi. In these diagrams, the red line represents the track of the typhoon; the blue dots represent high-voltage substations, and the pink and green lines represent 161 and 345 kV transmission lines, respectively. The triangles and crosses in Fig. 9 indicate the transmission lines that were disconnected from the main grid during the typhoon. Further details of these stages are as follows.

1) In the first stage, the radius of influence of Typhoon Megi was 50 km and the highest wind speed was 45 m/s. Fig. 8 shows the typhoon track in the first stage.
2) In the second stage, Typhoon Megi made landfall in Taiwan and its radius of influence was reduced to 30 km. In this stage, the highest wind speed was 35 m/s. Fig. 9 shows the typhoon track in the second stage.
3) In the third stage, according to the records, the radius of influence of Typhoon Megi was 10 km and the highest

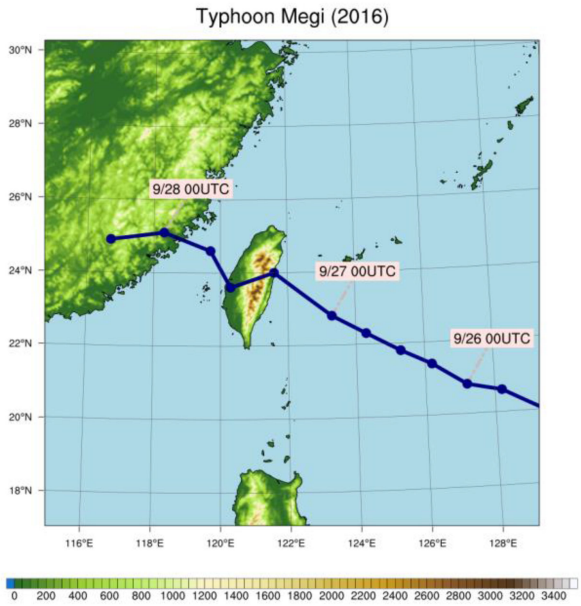

Fig. 7. Track of Typhoon Megi.

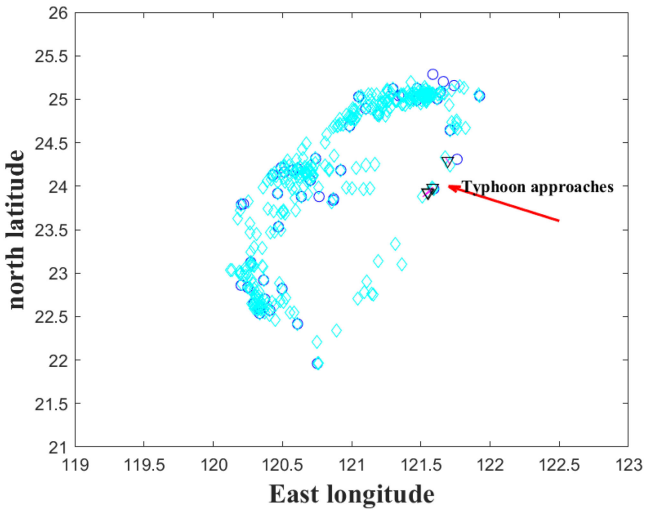

Fig. 8. First stage of Typhoon Megi.

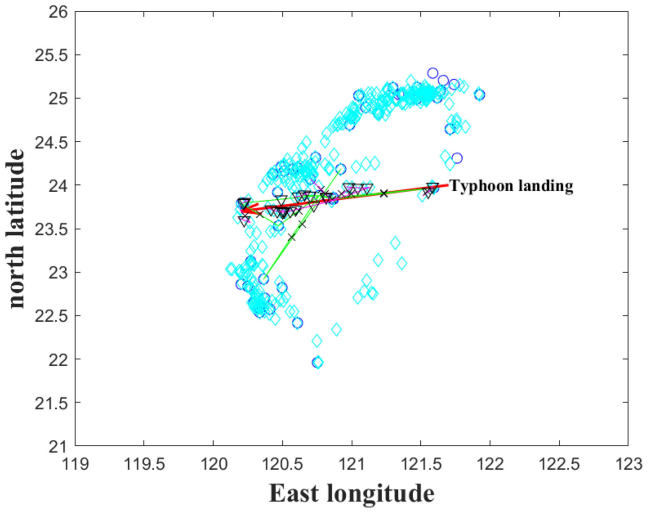

Fig. 9. Second stage of Typhoon Megi.

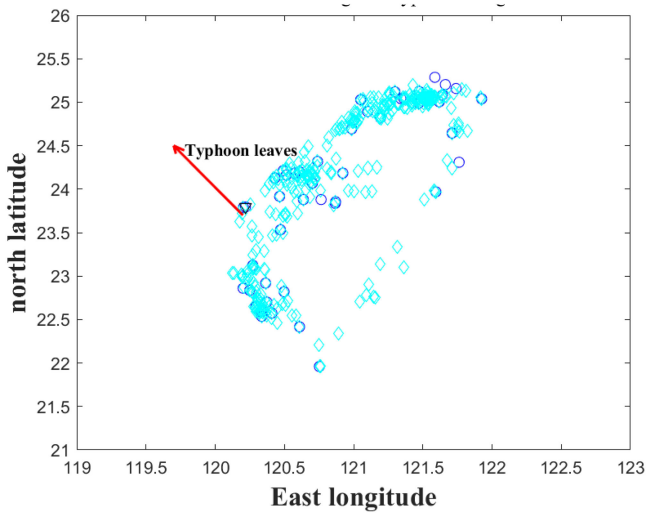

Fig. 10. Third stage of Typhoon Megi.

wind speed was 35 m/s. Fig. 10 shows the typhoon track in the third stage.

In the simulation, several transmission lines were disconnected from the main grid because of high wind speeds and the line failure rate was obtained according to the fragility curve (see Section II-A). Next, the recovery time was calculated after line outages. As transmission lines returned to normal, they were reconnected to the system immediately. This article assumed three operating scenarios in the power system during Typhoon Megi.

1) No preventive actions.
2) Preventive action with the redispatch of transmission lines.
3) Preventive action with the redispatch of generators.

In the simulation, the load data of the power system were recorded from the energy management system (EMS) of a Taiwanese power company (Taipower). In addition, this article implemented optimal unit scheduling for all generators.

Fig. 11 shows the system load curve during Typhoon Megi. The influence time (T_{dur}) of this typhoon (i.e., the typhoon land warning) was approximately 16 h, and the total influence time of the typhoon from approaching, landing, and leaving, to the complete recovery of the power system was approximately 81 h (from T_0 to T_5 in Fig. 5). The normal load curve in Fig. 11 was obtained from a similar day in the same month (September 2016), which was recorded in the EMS of Taipower. Based on the above three scenarios, this article calculated the resilience values using (3). The resilience value depends on the influence time of the typhoon, the level of power outage, and the recovery time of the power system. Table II gives the results for the resilience values in the three scenarios.

It is observed from Fig. 11 that the system loads under various operating scenarios are different. For instance, if a preventive action (either redispatching generators or redispatching transmission lines) is performed, then the system can meet a greater load demand and achieve a high resilience index. Furthermore, a preventive action with redispatching generators achieves a higher system resilience compared to redispatching transmission

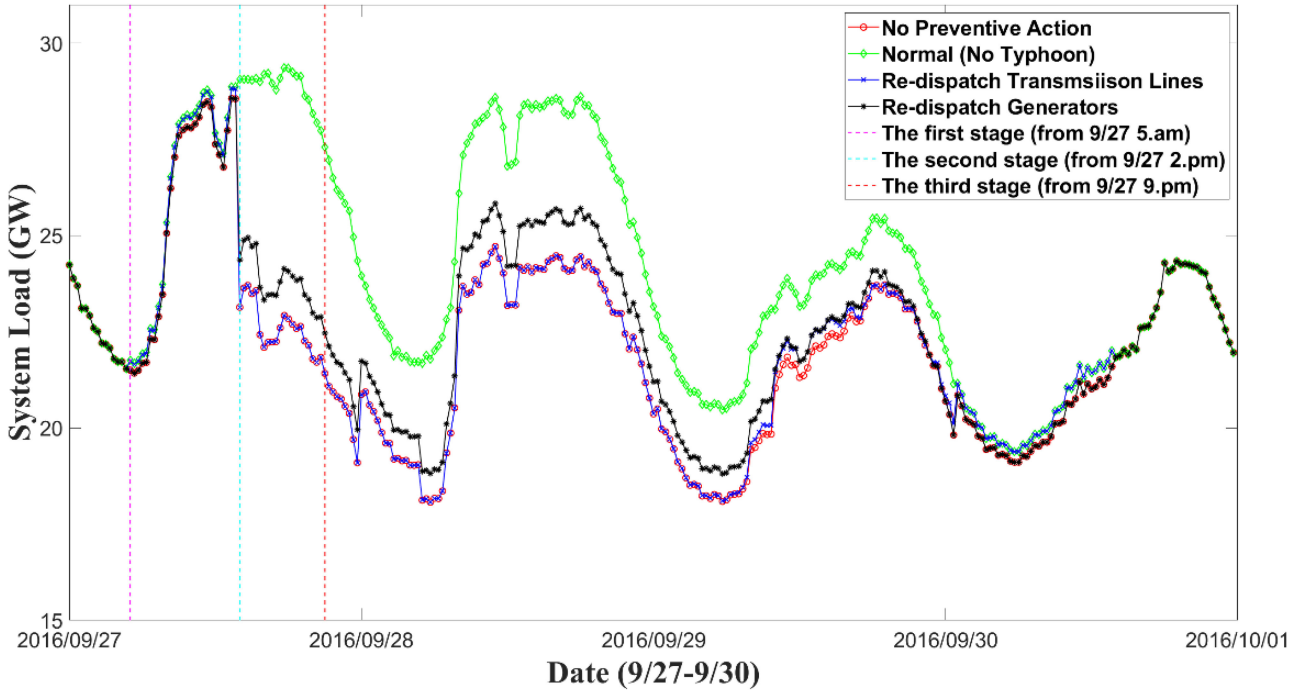

Fig. 11. System load over time.

TABLE II
CALCULATION OF RESILIENCE INDEX

$T_{dur} = 16hr$ $T_5 - T_0 = 81hr$ $T_{dur}/(T_5 - T_0) = 0.1975$			
Scenarios:	Scenario 1	Scenario 2	Scenario 3
$\frac{A_1 + A_2}{A_1 + A_2 + A_3}$	0.8905	0.8931	0.9136
Resilience Index	0.1759	0.1764	0.1805
Resilience Improvement	---	+ 0.0005	+ 0.0046

TABLE III
STRUCTURE OF ELECTRICAL LOAD IN TAIWAN

Residential	Industrial	Commercial	others
20.63%	55.82%	15.45%	8.1%

TABLE IV
AGGREGATED AVERAGE INTERRUPTION COST PER DAY

Category	Cost (NT$/kW)
Industrial consumers	40.95
Commercial consumers (Business)	27.71
Commercial consumers (Public utilities)	31.42

lines. The number of transmission lines is much greater than that of generators, with the result that transmission lines are more easily affected by typhoons. Therefore, if the radius of influence of a typhoon is large, preventive actions of system operators taken by redispatching transmission lines may not be very effective.

In this simulation, numerous local load demands were disconnected from the main grid because of transmission line outages, which resulted in islanding systems. A preventive action with redispatch of generators significantly reduces the amount of load loss. For instance, if an islanding system with some generators is expected to be disconnected from the main grid, then these local generators can be operated in a deloading mode before a typhoon strikes, and other remote generators can be redispatched to increase their power generation. Based on the simulation results in this article, a high resilience value can be achieved if the amount of redispatch generation exceeds 30% of the original generating pattern.

The next step in the proposed method is to calculate the economic value. First, it is necessary to calculate the value of the cost-loss ratio (also called prevention costs/protectable loss) for each operating scenario, in which "cost" means the required cost to take preventive actions, and "loss" indicates the avoidable cost if preventive actions are implemented. The protectable loss can be calculated based on the structure of different load types and their corresponding interruption costs. Table III gives the structure of electrical loads in Taiwan; industrial and commercial loads account for 70% of the total load. This article referred to [33] to obtain the interruption costs for different loads. Table IV gives the used interruption cost (the cost per kilowatt) for different load types.

The calculation of economic value by taking preventive actions is as follows.

TABLE V
TOTAL INTERRUPTION COST DURING TYPHOON MAGI

Category	Cost (NT$)
Electricity bill	25954173
Industrial	288554481.1
Commercial	115319339.1
Total	429827993.2

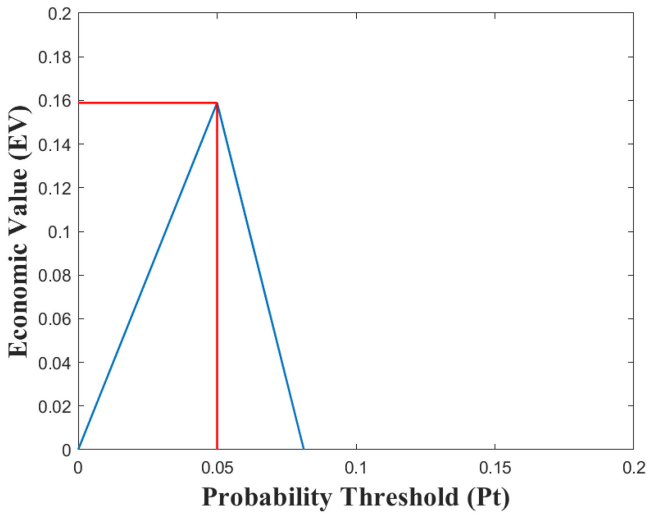

Fig. 12. Pt–EV curve based on the redispatch of transmission lines.

TABLE VI
INTERRUPTION COSTS

Category	COST(NT$/kWh)
Electricity bill	2.57
Industrial consumers	28.573
Commercial consumers	11.419
Prevention cost	1.77

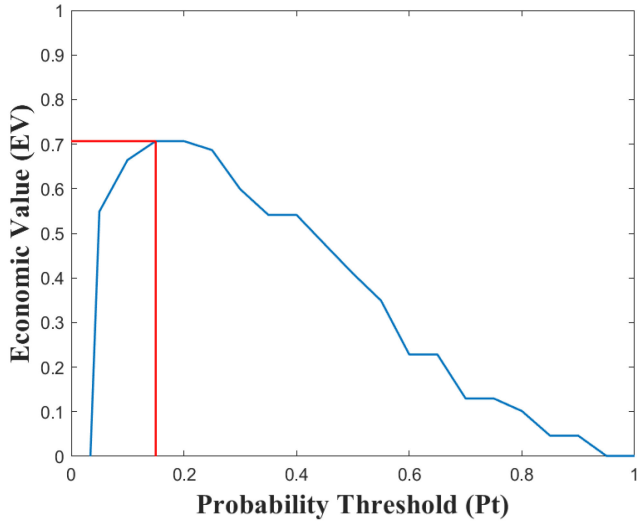

Fig. 13. Pt–EV curve based on the redispatch of generators.

1) Redispatch of Transmission Lines: With this preventive action, several transmission lines were redispatched in advance. Thus, when Typhoon Megi strikes Taiwan, this action avoids the disconnection of several load demands and reduces interruption costs. The line redispatch is decided by the predicted typhoon track and corresponding wind speeds. In this article, the required operating cost for line redispatch was assumed to be one million Taiwan dollars, which is based on historical records of the cost of labor. Table V gives the total interruption cost during Typhoon Magi. This includes the lost revenue and the interruption costs from industrial and commercial consumers.

The cost-loss ratio was subsequently calculated as 0.0023. Then, the maximum value of EV was found to be 0.1589, which indicates that the maximum cost saving is 0.1589 times the optimal cost of a perfect prediction.

In addition, the probability threshold (P_t) was obtained as 0.05. P_t is determined according to the maximum EV. It reveals that a preventive action should be implemented if the occurrence probability of a natural disaster exceeds the value of P_t. Based on this result, it is suggested that, when the probability of NWP wind speeds above 45 m/s exceeds 5%, preventive actions should be taken to achieve the best economic benefit. Fig. 12 shows the derived Pt–EV curve using the preventive action of redispatching transmission lines.

2) Redispatch of Generators: With this preventive action, several generators were redispatched in advance. That is, the output of generators located in the islanding systems caused by the typhoon should be reduced before the typhoon strikes. Thus, when Typhoon Megi strikes Taiwan, this action avoids the interruption of several load demands and reduces interruption costs. The required cost for this preventive action is based on the generator redispatch cost. In this case study, the actual unit scheduling and generator redispatch in the Taiwan power system were implemented, and the cost of protectable loss was calculated based on the interruption cost. Table VI gives the detailed interruption cost, including the lost revenue and the interruption costs from industrial and commercial consumers. In this case study, the average generation cost for redispatching generators was 1.77 (NT$/kWh).

The calculated cost-loss ratio was 0.0415. EV was 0.7068, and the probability threshold (P_t) was 0.15. That means when the probability of NWP wind speeds above 45m/s exceeds 15%, it is suggested that preventive action be taken to achieve the best economic benefits. Fig. 13 shows the Pt–EV curve using the preventive action of redispatching generators.

To compare the differences between the two preventive actions, Table VII gives the economic value and probability thresholds for the two preventive operations. The action of redispatching generators clearly achieves a higher economic benefit compared to the action of redispatching transmission lines, but

TABLE VII
COMPARISON OF TWO PREVENTIVE ACTION OPERATIONS

Item	Re-dispatch of transmission lines	Re-dispatch of generators
EV	0.1589	0.7068
Pt	5%	15%

TABLE VIII
COMBINATION OF RESILIENCE VALUE AND ECONOMIC VALUE

	No preventive actions are taken	Re-dispatch of transmission lines	Re-dispatch of generators
Resilience Value	0.1759	0.1764	0.1805
Resilience improvement	---	+ 0.0005	+ 0.0046
Economic Value	---	0.1589	0.7068
Economic Value (pu)	---	$\frac{0.1589}{1.589} = 0.1$	$\frac{0.7068}{7.068} = 0.1$
Integration between Resilience and EV	---	$\frac{0.0005}{1.589} = 3.15 \times 10^{-4}$	$\frac{0.0046}{7.068} = 6.51 \times 10^{-4}$

this decision should be made if the probability of NWP wind speeds above 45 m/s is over 15%.

This article considers both resilience value and economic value to make decisions for preventive actions [34]. If economic values using different preventive actions are transferred to 0.1 p.u., then it is possible to observe how much the resilience can be improved for every 0.1 unit of economic value. Table VIII gives the results. It is evident from this table that the preventive action by redispatching generators surpasses that by redispatching transmission lines because the resilience under the same economic-value unit is high. This enables system operators to select the redispatch of generators as a high priority for preventive actions and thus maximize the ability of the system to respond to typhoons.

V. CONCLUSION

With climate change, power systems face increasingly severe natural disasters. It is thus vital to improve power system resilience to cope with high-impact low-probability events. This article analyzed the robustness of a power system through the calculation of resilience and considered two kinds of preventive actions to enhance power system resilience. The simulation results demonstrated that it is possible to reduce the interruption cost if appropriate preventive actions are implemented. In addition to the consideration of power system resilience, economic value should also be analyzed to reveal the potential economic benefits of implementing preventive actions. Thus, this article proposed a process to calculate economic value by considering NWPs of wind speeds, prevention cost, and the cost of protectable loss. A high economic value indicates that the implemented preventive action is effective because it achieves a high cost saving. Furthermore, this article provided a probability threshold for determining when to begin taking preventive actions. When the predicted wind speeds exceed the probability threshold, it is recommended that preventive action be implemented.

By combining resilience and economic values, system operators can select appropriate preventive actions to improve power system resilience with the maximum economic benefit. A comprehensive consideration provides high system resilience at the least cost, under the influence of a severe weather event, such as a typhoon. Based on the proposed method, power system operators can make the best decisions for preventive actions when an extreme weather event occurs.

REFERENCES

[1] B. L. Preston *et al.*, *Resilience of the US Electricity System: A Multi-Hazard Perspective*. Washington, DC, USA: US Dept. Energy Office Policy, 2016.
[2] H. Raoufi, V. Vahidinasab, and K. Mehran, "Power systems resilience metrics: A comprehensive review of challenges and outlook," *Sustainability,* vol. 12, no. 22, 2020, Art. no. 9698.
[3] B.-J. Jesse, H. U. Heinrichs, and W. Kuckshinrichs, "Adapting the theory of resilience to energy systems: A review and outlook," *Energy, Sustain. Soc.,* vol. 9, no. 1, pp. 1–19, 2019.
[4] M. Ouyang, L. Dueñas-Osorio, and X. Min, "A three-stage resilience analysis framework for urban infrastructure systems," *Struct. Saf.,* vol. 36, pp. 23–31, 2012.
[5] Z. Bie, Y. Lin, G. Li, and F. Li, "Battling the extreme: A study on the power system resilience," *Proc. IEEE,* vol. 105, no. 7, pp. 1253–1266, Apr. 2017.
[6] N. Bhusal, M. Abdelmalak, M. Kamruzzaman, and M. Benidris, "Power system resilience: Current practices, challenges, and future directions," *IEEE Access,* vol. 8, pp. 18064–18086, Jan. 2020.
[7] Y. Yang, W. Tang, Y. Liu, Y. Xin, and Q. Wu, "Quantitative resilience assessment for power transmission systems under typhoon weather," *IEEE Access,* vol. 6, pp. 40747–40756, Jul. 2018.
[8] X. Liu *et al.*, "A resilience assessment approach for power system from perspectives of system and component levels," *Int. J. Elect. Power,* vol. 118, 2020, Art. no. 105837.
[9] H. Chen, F. S. Bresler, III, M. E. Bryson, K. Seiler, J. Monken, and E. Magazine, "Toward bulk power system resilience: Approaches for regional transmission operators," *IEEE Power,* vol. 18, no. 4, pp. 20–30, Jun. 2020.
[10] S. Kosai and J. Cravioto, "Resilience of standalone hybrid renewable energy systems: The role of storage capacity," *Energy,* vol. 196, 2020 , Art. no. 117133.
[11] M. Nazemi, M. Moeini-Aghtaie, M. Fotuhi-Firuzabad, and P. Dehghanian, "Energy storage planning for enhanced resilience of power distribution networks against earthquakes," *IEEE Trans. Sustain. Energy,* vol. 11, no. 2, pp. 795–806, Mar. 2019.
[12] H. Lee *et al.*, "An energy management system with optimum reserve power procurement function for microgrid resilience improvement," *IEEE Access,* vol. 7, pp. 42577–42585, Mar. 2019.
[13] E. Rosales-Asensio, M. de Simón-Martín, D. Borge-Diez, J. J. Blanes-Peiró, and A. Colmenar-Santos, "Microgrids with energy storage systems as a means to increase power resilience: An application to office buildings," *Energy,* vol. 172, pp. 1005–1015, 2019.
[14] A. Hussain, V.-H. Bui, and H.-M. Kim, "Microgrids as a resilience resource and strategies used by microgrids for enhancing resilience," *Appl. energy,* vol. 240, pp. 56–72, 2019.
[15] M. Ayar, S. Obuz, R. D. Trevizan, A. S. Bretas, and H. A. Latchman, "A distributed control approach for enhancing smart grid transient stability and resilience," *IEEE Trans. Smart Grid,* vol. 8, no. 6, pp. 3035–3044, Jun. 2017.
[16] A. Hussain, V.-H. Bui, and H.-M. Kim, "Resilience-oriented optimal operation of networked hybrid microgrids," *IEEE Trans. Smart Grid,* vol. 10, no. 1, pp. 204–215, Aug. 2017.

[17] M. Borghei, M. J. I. J.o. E. P. Ghassemi, and E. Systems, "Optimal planning of microgrids for resilient distribution networks," *Int. J. Elect. Power Energy Syst.*, vol. 128, pp. 106682, 2021.

[18] Q. Wang, Z. Yu, R. Ye, Z. Lin, and Y. Tang, "An ordered curtailment strategy for offshore wind power under extreme weather conditions considering the resilience of the grid," *IEEE Access,* vol. 7, pp. 54824–54833, Apr. 2019.

[19] D. N. Trakas and N. D. Hatziargyriou, "Resilience constrained day-ahead unit commitment under extreme weather events," *IEEE Trans. Power Syst.,* vol. 35, no. 2, pp. 1242–1253, Oct. 2019.

[20] H. S. Dhiman, D. Deb, S. Muyeen, and I. Kamwa, "Wind turbine gearbox anomaly detection based on adaptive threshold and twin support vector machines," *IEEE Trans. Energy Convers.*, vol. 36, no. 4, pp. 3462–3469, Dec. 2021.

[21] T. Ding, M. Qu, Z. Wang, B. Chen, C. Chen, and M. Shahidehpour, "Power system resilience enhancement in typhoons using a three-stage day-ahead unit commitment," *IEEE Trans. Smart Grid*, vol. 12, no. 3, pp. 2153–64, Dec. 2020.

[22] Y. Li, K. Xie, L. Wang, and Y. Xiang, "Exploiting network topology optimization and demand side management to improve bulk power system resilience under windstorms," *Elect. Power Syst. Res.,* vol. 171, pp. 127–140, 2019.

[23] H. Momen, A. Abessi, S. Jadid, M. Shafie-khah, and J. P. Catalão, "Load restoration and energy management of a microgrid with distributed energy resources and electric vehicles participation under a two-stage stochastic framework," *Int. J. Elect. Power Energy Syst.*, vol. 133, 2021, Art. no. 107320.

[24] H. Ranjbar, S. H. Hosseini, and H. Zareipour, "Resiliency-Oriented planning of transmission systems and distributed energy resources," *IEEE Trans. Power Syst.*, vol. 36, no. 5, pp. 4114–4125, Mar. 2021.

[25] H.-L. Chang, S.-C. Yang, H. Yuan, P.-L. Lin, and Y.-C. Liou, "Analysis of the relative operating characteristic and economic value using the LAPS ensemble prediction system in Taiwan," *Monthly Weather Rev.,* vol. 143, no. 5, pp. 1833–1848, 2015.

[26] R. W. Katz and A. H. Murphy, *Economic Value of Weather and Climate Forecasts*. Cambridge, U.K.: Cambridge Univ. Press, 2005.

[27] K. Mylne, "The use of forecast value calculations for optimal decision making using probability forecasts," in *Proc.17th Conf. Weather Anal. Forecasting*, 1999.

[28] D. S. Richardson, "Measures of skill and value of ensemble prediction systems, their interrelationship and the effect of ensemble size," *Quart. J. Roy. Meteorol. Soc.,* vol. 127, no. 577, pp. 2473–2489, 2001.

[29] D. S. Richardson, "Skill and relative economic value of the ECMWF ensemble prediction system," *Quart. J. Roy. Meteorol. Soc.,* vol. 126, no. 563, pp. 649–667, 2000.

[30] D. S. Wilks and T. M. Hamill, "Potential economic value of ensemble-based surface weather forecasts," *Monthly weather Rev.,* vol. 123, no. 12, pp. 3565–3575, 1995.

[31] Y. Zhu, Z. Toth, R. Wobus, D. Richardson, and K. Mylne, "The economic value of ensemble-based weather forecasts," *Bull. Amer. Meteorol. Soc.,* vol. 83, no. 1, pp. 73–84, 2002.

[32] M. Sullivan, M. T. Collins, J. Schellenberg, and P. H. Larsen, "Estimating power system interruption costs: A guidebook for electric utilities," 2018.

[33] E. Dialynas, S. Megaloconomos, and V. Dali, "Interruption cost analysis for the electrical power customers in Greece," in *Proc. 16th Int. Conf. Exhib. Electricity Distrib. Part 1, Contribution*, 2001.

[34] Y. -K. Wu, Y. -C. Chen, H. -L. Chang, and J. -S. Hon, "The effect of decision analysis on power system resilience and economic value during a severe weather event," in *Proc. IEEE Ind. Appl. Soc. Annu. Meeting*, Oct. 2021, pp. 1–10, doi: 10.1109/IAS48185.2021.9677422.